Electronic Supplementary Material (ESI) for Journal of Materials Chemistry A.

<Electronic Supplementary Information>

Two-step Growth of $CsPbI_{3-x}Br_x$ Films Employing Dynamic CsBr Treatment: Toward All-inorganic Perovskite Photovoltaics with Enhanced Stability

Bhaskar Parida [1)], Jun Ryu [1)], Saemon Yoon [1)], Seojun Lee [1)], Yejin Seo [1)], Jung Sang Cho [2)], and Dong-Won Kang [1,*)]

[1)] *School of Energy Systems Engineering, Chung-Ang University, Seoul 06974, Republic of Korea*

[2)] *Department of Engineering Chemistry, Chungbuk National University, 28644, Republic of Korea*

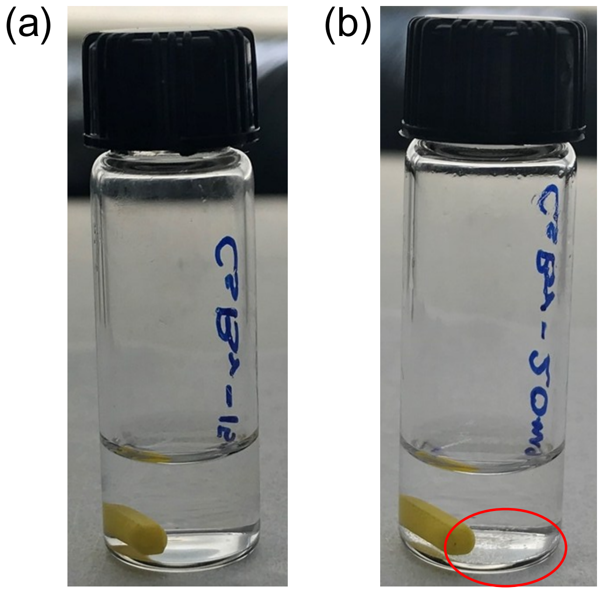

Figure S1. Photographic images showing the solubility of (a) 15 mg and (b) 20 mg CsBr in 1 mL of methanol.

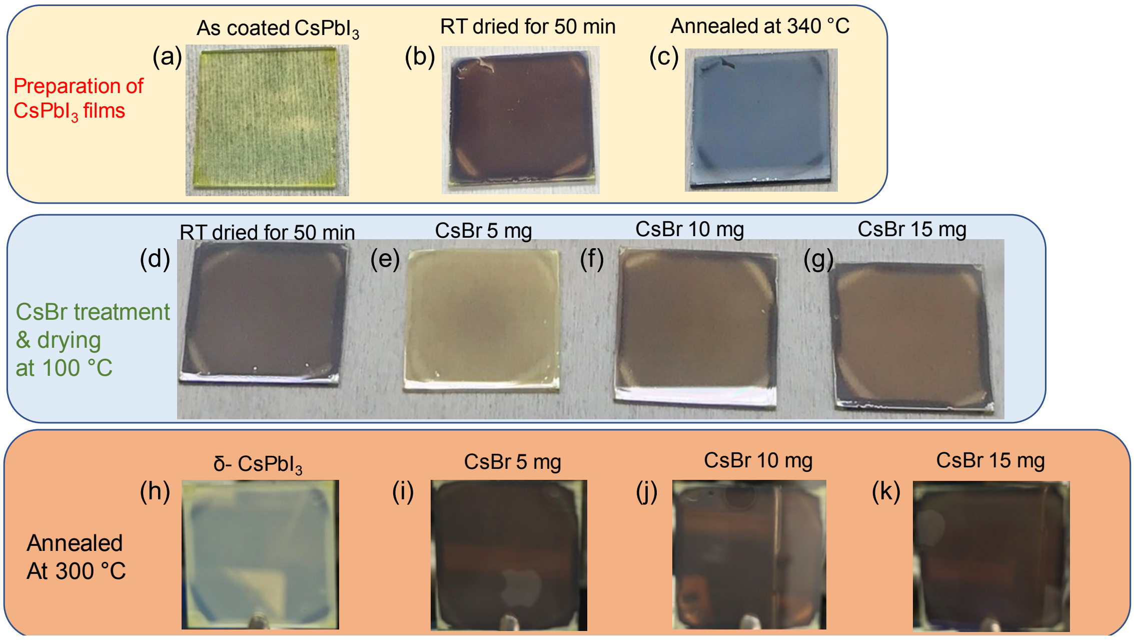

Figure S2. Photographic images of the fabrication process for α-$CsPbI_{3-x}Br_x$ perovskite films (a-c) without and (e-g) with a dynamic coating of various concentrations of CsBr (5–15 mg) and drying at 100 °C and (i-k) annealing at 300 °C. (d) The α-$CsPbI_3$ film prepared using room temperature (RT) drying that (h) degraded to δ-$CsPbI_3$ after annealing at 300 °C.

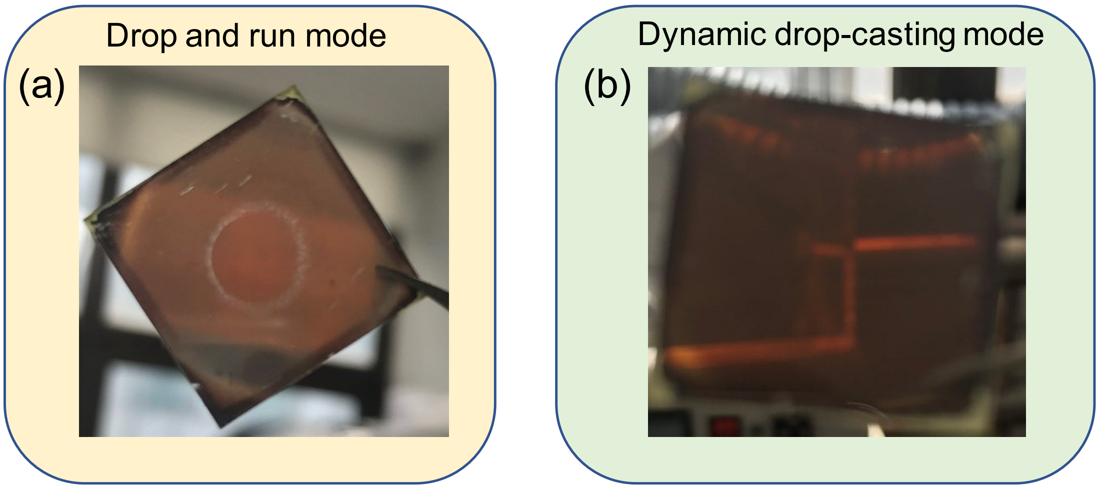

Figure S3. Photographic images of α-$CsPbI_{3-x}Br_x$ perovskite films prepared using the (a) drop and run and (b) dynamic drop-casting of a 15-mg CsBr solution.

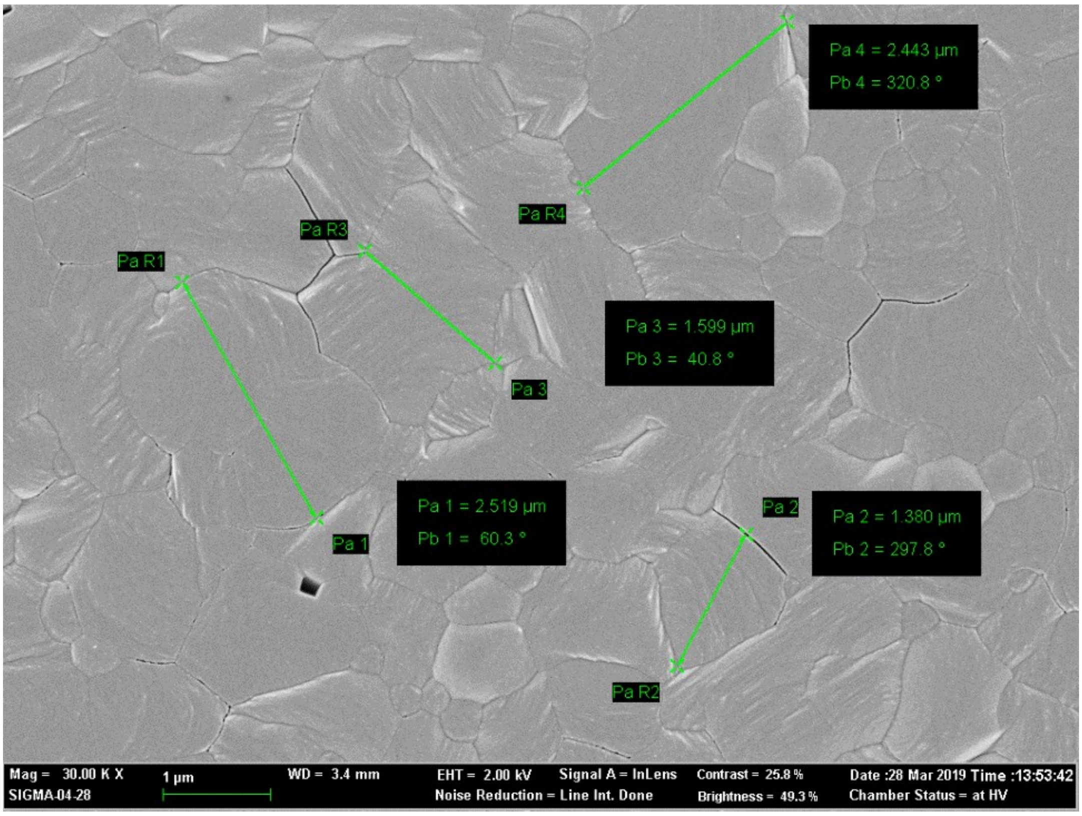

Figure S4. Top-view FE-SEM images of CsBr-15 perovskite film with grain sizes over 2 µm.

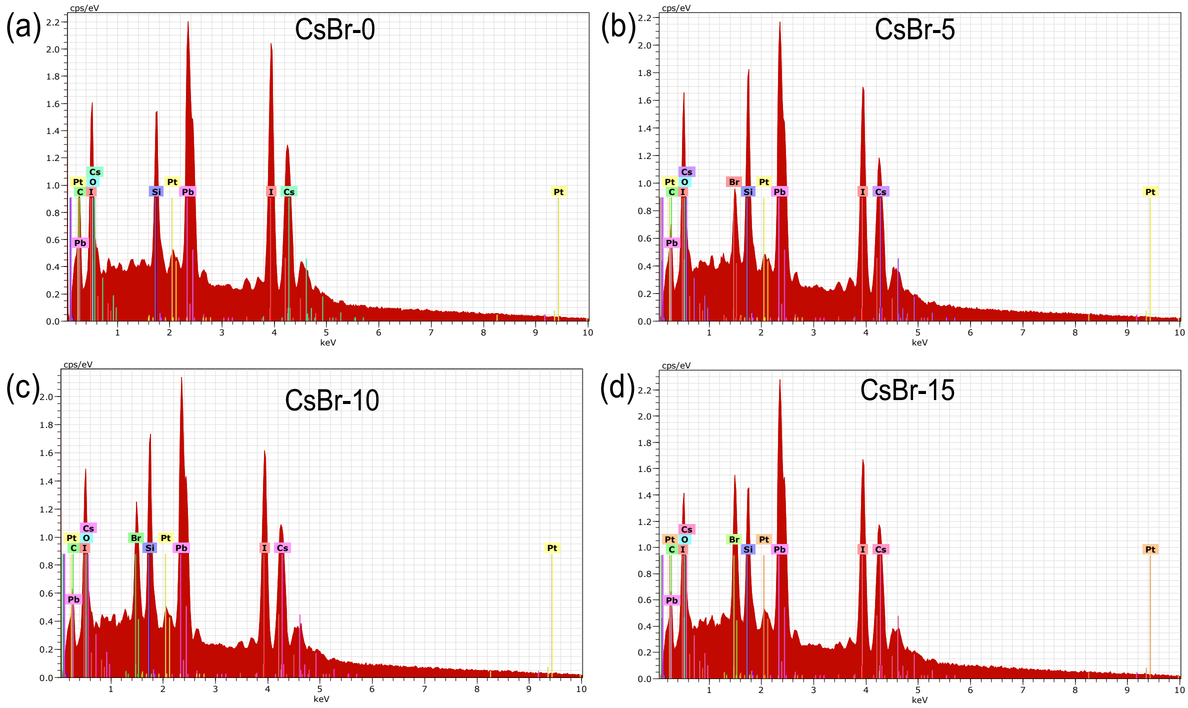

Figure S5. EDX spectra of the (a) CsBr-0, (b) CsBr-5, (c) CsBr-10, and (d) CsBr-15 perovskite films prepared with and without a dynamic CsBr coating.

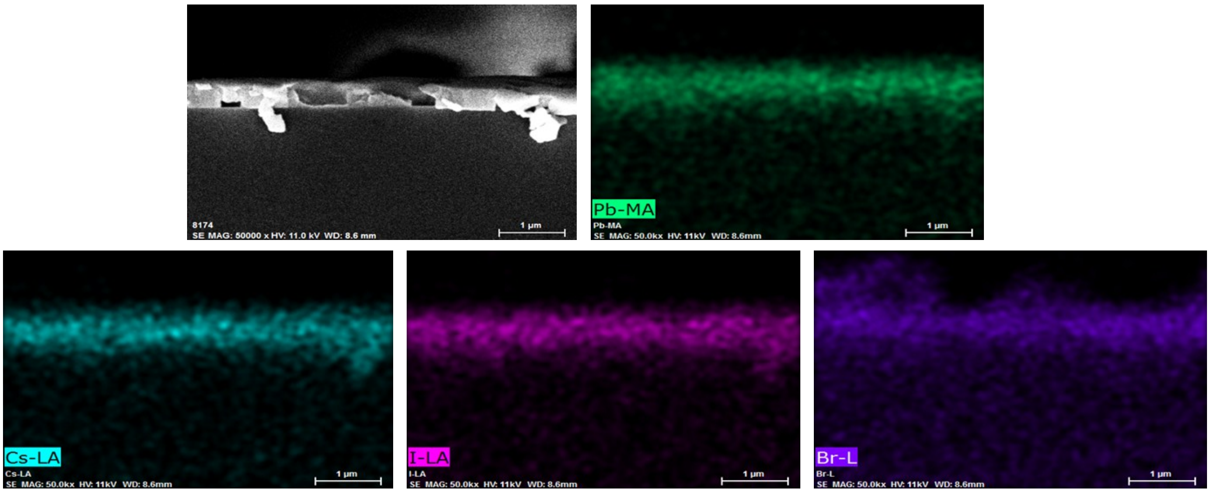

Figure S6. Cross-sectional EDX mapping profile of the CsBr-15 perovskite film.

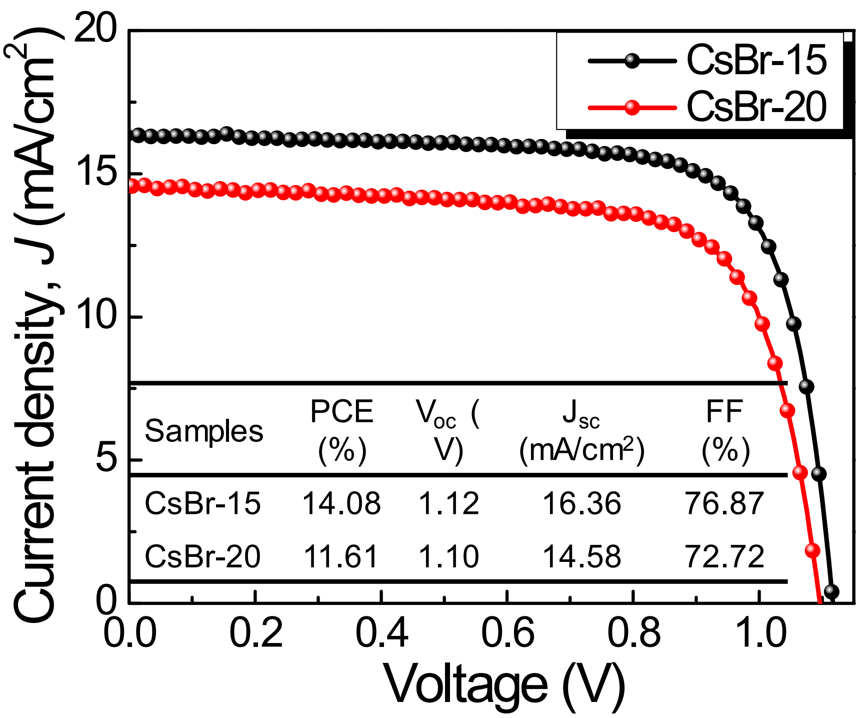

Figure S7. J–V characteristic curves for the $CsPbI_{3-x}Br_x$ inorganic PSCs fabricated with a dynamic CsBr coating using the increased precursor concentration (20 mg/mL, heated at 50 °C) as well as the property of the champion CsBr-15 device (CsBr 15 mg/mL at room temperature).

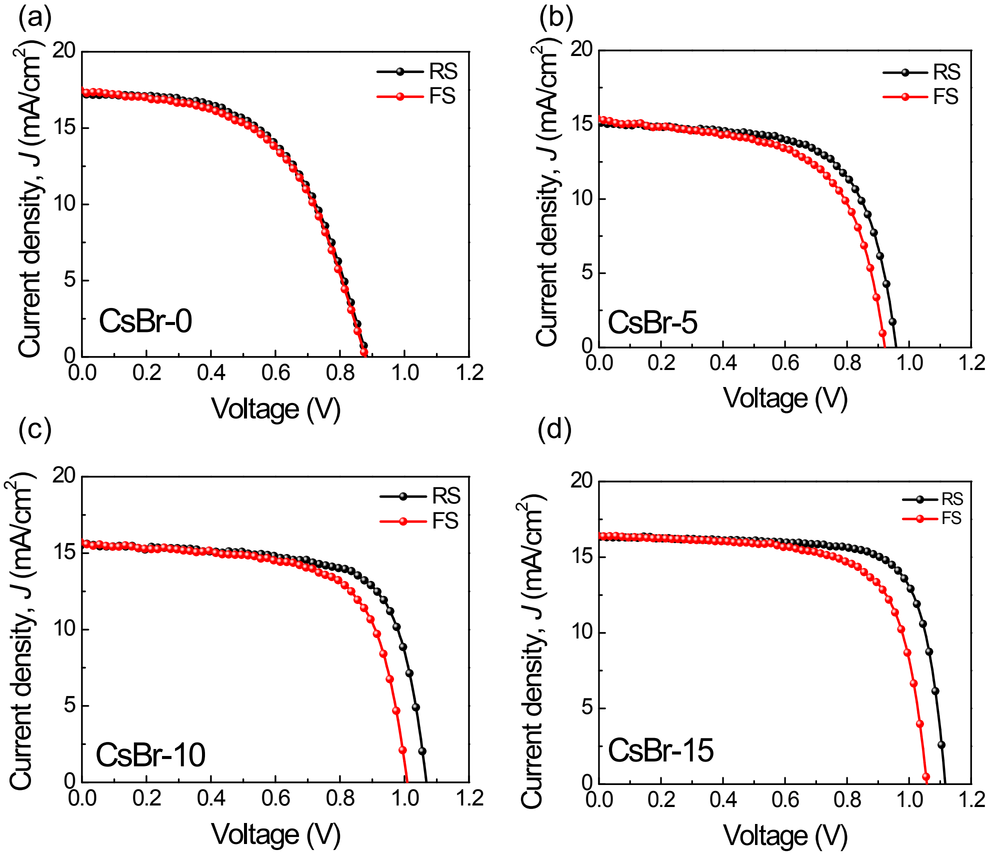

Figure S8. Hysteresis behavior of the $CsPbI_{3-x}Br_x$ PSCs fabricated (a) without CsBr and (b-d) with dynamic CsBr-5, CsBr-10, and CsBr-15 coatings as revealed by reverse and forward scans.

Table S1. Hysteresis behavior of the $CsPbI_{3-x}Br_x$ PSCs fabricated (a) without CsBr and (b-d) with dynamic treatment CsBr-5, CsBr-10, and CsBr-15 coatings as revealed by reverse and forward scans.

Sample	Direction	PCE (%)	V_{oc} (V)	J_{sc} (mA/cm^2)	FF (%)
CsBr-0	RS	8.40	0.88	17.20	56.47
	FS	8.33	0.87	17.44	54.69
CsBr-5	RS	9.63	0.96	15.23	66.02
	FS	8.66	0.92	15.58	60.46
CsBr-10	RS	11.81	1.06	15.54	71.33
	FS	10.66	1.01	15.88	66.77
CsBr-15	RS	14.08	1.12	16.36	76.87
	FS	12.18	1.06	16.29	69.90

Table S2. A summary of stability results on recently reported inorganic PSCs.

Ref. No.	**Device structure**	**Temp. (°C)**	**R.H. (%)**	**Initial PCE (%)**	**PCE Decay (%)**	**Storage Time (h)**
			N_2 atmosphere			
R2.1	ITO/ZnO/ $Cs_{1.2}PbI_2Br_{1.2}$ /P3HT/Au	70	< 20	9.8	30	500
R2.2	FTO/NiMgLiO/$CsPbI_2Br$/PCBM/BCP/Ag	85	< 20	9.14	10	500
R2.3	FTO/PTAA/$CsPbI_3$/ PCBM/BCP/Ag	RT	< 10	13.32	15	720
R2.4	FTO/TiO_2/$CsPbI_3$-PTABr/Spiro-OMeTAD/Au	RT	< 10	17.06	9	500
Our work	ITO/TiO_2/$CsPbI_{3-x}Br_x$/P3HT/Au	RT	<10	14.08	30	1200
			Air atmosphere			
R2.5	FTO/TiO_2/ $Cs_{0.925}K_{0.075}PbI_2Br$ / Spiro-OMeTAD/Au	RT	20	10.0	20	144
[24]	FTO/TiO_2/ $CsPbI_{2.98}Br_{0.2}$/Spiro-OMeTAD/Au	RT	20	10.92	0	192
R2.6	FTO/TiO_2/$CsPbIBr_2$ /Spiro-OMeTAD/Au	RT	25	7.31	50	100
[14]	FTO/TiO_2/$CsPb_{0.96}Bi_{0.04}I_3$/CuI/Au	RT	55	13.21	32	168
R2.7	FTO/TiO_2/$CsPbI_3$ QDs/Spiro-OMeTAD/MoO_x/Al	RT	40-60	10.77	74	48
Our work	ITO/TiO_2/$CsPbI_{3-x}Br_x$/P3HT/Au	85	40	14.08	0	48

[R2.1] L. A. Frolova, Q. Chang, S. Y. Luchkin, D. Zhao, A. F. Akbulatov, N. N. Dremova, A. V. Ivanov, E. E. M. Chia, K. J. Stevenson and P. A. Troshin, Efficient and stable all-inorganic perovskite solar cells based on nonstoichiometric $Cs_xPbI_2Br_x$ (x > 1) alloys, J. Mater. Chem. C, 2019,**7**, 5314-5323.

[R2.2] S. Zhang, S. Wu, W. Chen, H. Zhu, Z. Xiong, Z. Yang, C. Chen, R. Chen, L. Han and W. Chen, Solvent engineering for efficient inverted perovskite solar cells based on inorganic $CsPbI_2Br$ light absorber, Materials Today Energy 2018, 8, 125-133.

[R2.3] T. Wu, Y. Wang, Z. Dai, D. Cui, T. Wang, X. Meng, E. Bi, X. Yang, and L. Han, Efficient and Stable CsPbI3 Solar Cells via Regulating Lattice Distortion with Surface Organic Terminal Groups, Adv. Mater. 2019, 1900605.

[R2.4] Y. Wang, T. Zhang, M. Kan, Y. Zhao, Bifunctional Stabilization of All-Inorganic α-$CsPbI_3$ Perovskite for 17% Efficiency Photovoltaics, Journal of the American Chemical Society, 140 (2018) 12345-12348.

[R2.5] J.K. Nam, S.U. Chai, W. Cha, Y.J. Choi, W. Kim, M.S. Jung, J. Kwon, D. Kim, J.H. Park, Potassium Incorporation for Enhanced Performance and Stability of Fully Inorganic Cesium Lead Halide Perovskite Solar Cells, Nano Letters, 17 (2017) 2028-2033.

[R2.6] J. Lu, S-C. Chen, and Q. Zheng, Defect Passivation of $CsPbIBr_2$ Perovskites for High-Performance Solar Cells with Large Open-Circuit Voltage of 1.28 V, ACS Appl. Energy Mater. 2018, 1, 5872−5878.

[R2.7] A. Swarnkar, A.R. Marshall, E.M. Sanehira, B.D. Chernomordik, D.T. Moore, J.A. Christians, T. Chakrabarti, J.M. Luther, Quantum dot–induced phase stabilization of α-$CsPbI_3$ perovskite for high-efficiency photovoltaics, Science, 354 (2016) 92-95.

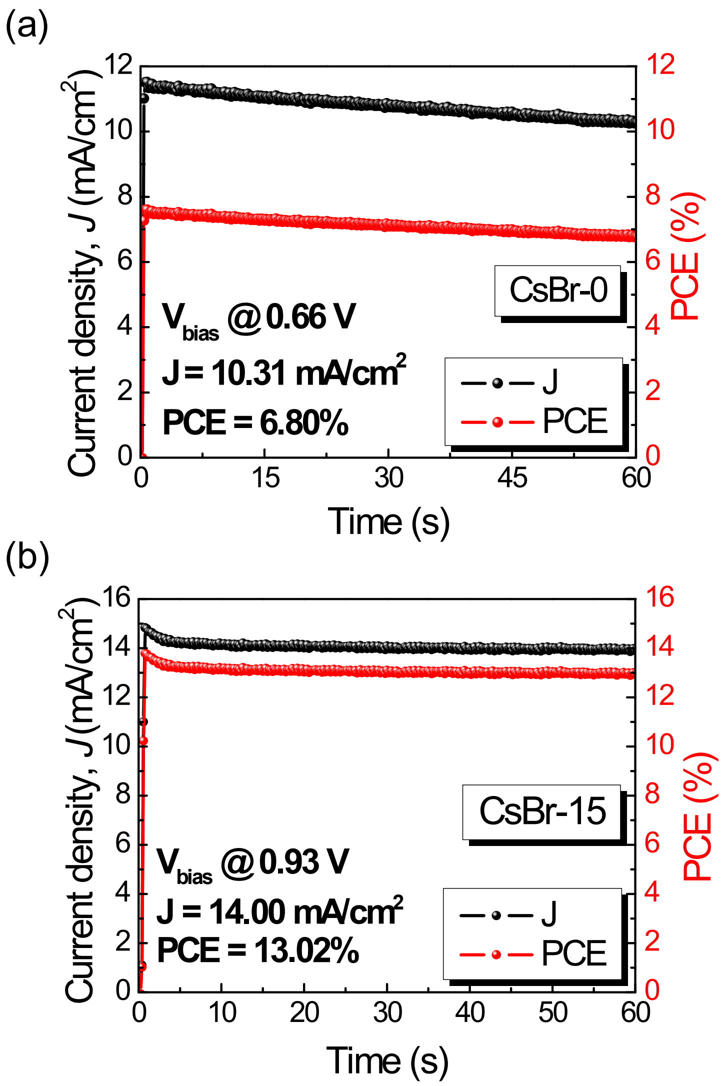

Figure S9. Stabilized photocurrent and PCE of the (a) CsBr-0 and (b) CsBr-15 inorganic PSCs.

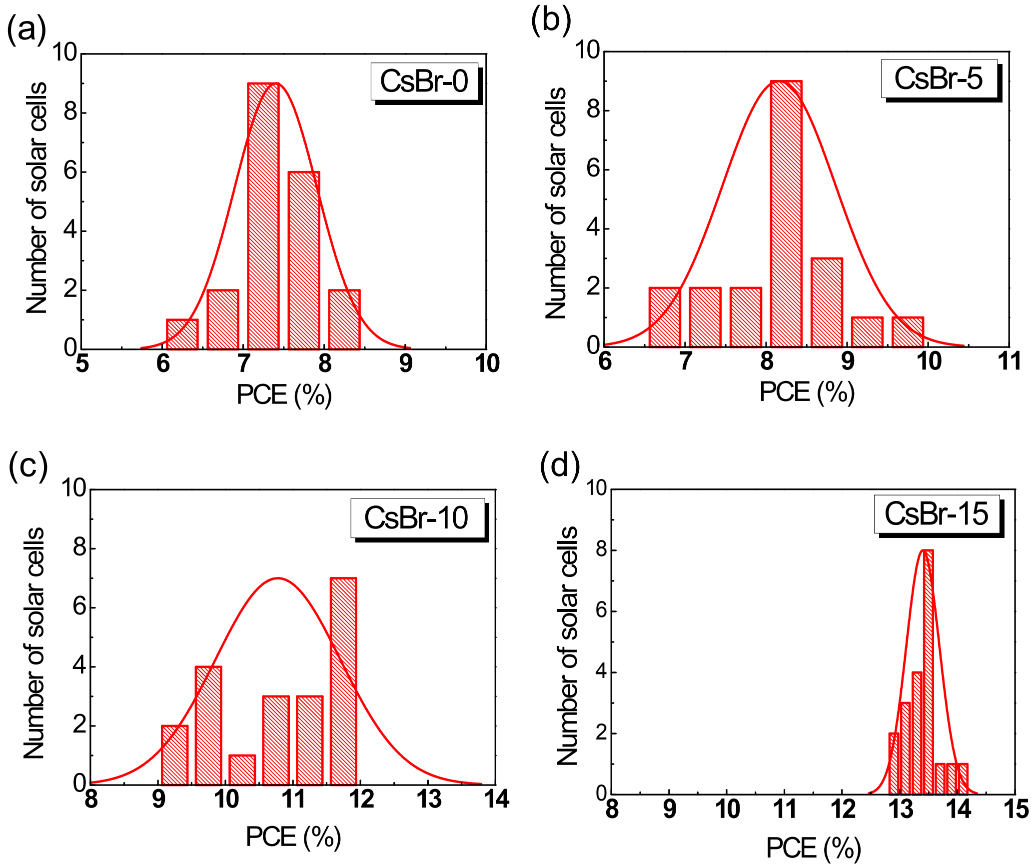

Figure S10. PCE distribution histograms for 20 devices of the $CsPbI_{3-x}Br_x$ PSCs fabricated (a) without CsBr (CsBr-0, $CsPbI_3$) and (b-d) with dynamic CsBr-5, CsBr-10, and CsBr-15 treatment.

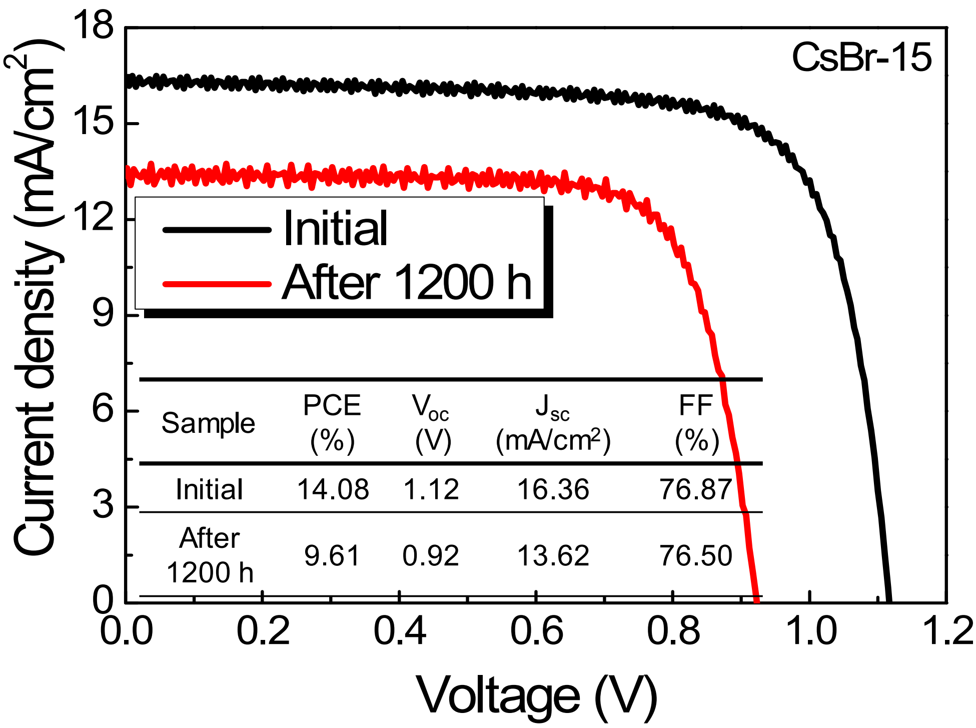

Sample	PCE (%)	V_{oc} (V)	J_{sc} (mA/cm^2)	FF (%)
Initial	14.08	1.12	16.36	76.87
After 1200 h	9.61	0.92	13.62	76.50

Figure S11. J-V curves (measured in atmospheric air ambient) of the unencapsulated CsBr-15 all-inorganic perovskite solar cells stored in a nitrogen-ambient for over 1200 h. The inset table presents the performance of fresh and stored devices.

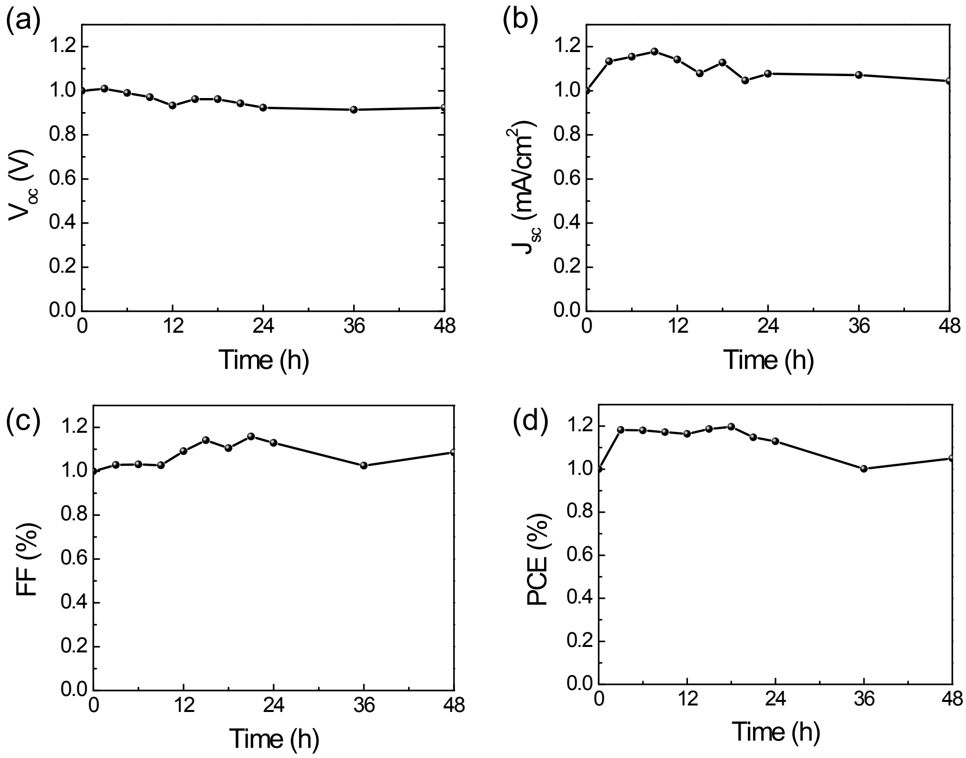

Figure S12. Normalized (a) V_{oc}, (b) J_{sc} (c) FF, and (d) PCE as a function of time for the CsBr-15 PSC without encapsulation, measured under ambient air at the temperature of 85 °C and RH of 40% for 48 h.